Acta Metall. Sin. (Engl. Lett.), 2014, **27**(6), 988–994
DOI 10.1007/s40195-014-0112-9

Preparation of Square and Labyrinth-Like TiO_2 Particles for Photo-Degradation of Organic Pollutants

Yongjie Yan · Shasha Zhang · Guohua Jiang · Xia Li · Zhen Wei · Wenxing Chen · Junmin Wan

Received: 18 November 2013 / Revised: 21 March 2014 / Published online: 19 July 2014

Abstract Square and labyrinth-like titanium dioxide particles were successfully synthesized by a simple hydrothermal method with assistant of halloysite nanotubes. The morphology and microstructure of as-prepared photo-catalysts were characterized by X-ray powder diffraction, scanning electron microscopy, transmission electron microscopy, and X-ray photoelectron spectroscopy. The photo-catalytic activity of as-prepared catalysts was evaluated by degradation of organic pollutants (Rhodamine B, methylene blue and methanol) under UV light irradiation.

KEY WORDS: Microstructure; Photolysis; Decomposition

1 Introduction

Anatase titanium oxide (TiO_2), one of the most investigated photo-catalytic materials, has been considered to have important application in pollutant degradation due to its unique properties such as quantum confinement, high specific surface area, and nontoxicity [1–4]. In order to obtain higher catalytic degradation ability, TiO_2 nanostructures with various morphologies, such as nanorods, nanoparticles, nanotubes, and micro/nano spheres have been received much attention in the past few years [5–12]. For example, hollow TiO_2 spheres have been prepared by the deposition of an inorganic coating of TiO_2 on the surface of the carbon spheres and subsequent removal of the carbon spheres templates by calcination in air. The hollow TiO_2 spheres can achieve 1.35 times higher phenol removal rate than that of P-25 under UV irradiation [5]. The hollow TiO_2 microspheres (HTS) composed of anatase polyhedra with exposed ~20% {001} facets exhibit tunable photo-catalytic selectivity in decomposing azo dyes in water [6]. Hollow TiO_2 particles prepared through calcination of the PSt/TiO_2 core–shell particles to burn off the PSt core or through dissolution of the core by tetrahydrofuran (THF) also show a much higher catalytic activity for the photo-degradation of Rhodamine B (RhB) [7]. Recently, hollow TiO_2 nanocages with rubik-like structure have been successfully developed in our group via a combined hydrolysis/hydrothermal method. Under UV irradiation, 99.9% phenol could be decomposed within 3 h by the obtained TiO_2 as a catalyst compared with approximately 70% degradation using P-25 [8]. Herein, the square and biscuit-like TiO_2 particles were prepared by a hydrothermal synthesis route with the assistance of HNTs and HF. Compared with P-25, the as-synthesized TiO_2 exhibited higher catalytic performance for the degradation of organic pollutions under UV light irradiation.

Available online at http://link.springer.com/journal/40195

Y. Yan · S. Zhang · G. Jiang
Qixin Honours College, Zhejiang Sci-Tech University, Hangzhou 310018, China

G. Jiang · X. Li · Z. Wei · W. Chen
Key Laboratory of Advanced Textile Materials and Manufacturing Technology (ATMT), Ministry of Education, Zhejiang Sci-Tech University, Hangzhou 310018, China

G. Jiang (✉) · X. Li · Z. Wei · W. Chen · J. Wan
Department of Materials Engineering, Zhejiang Sci-Tech University, Hangzhou 310018, China
e-mail: ghjiang_cn@zstu.edu.cn

2 Experimental

2.1 Materials

Halloysite nanotubes (HNTs) were purchased from Wenzhou Xincheng Shenfei Aluminum Alloy Co. Ltd. Pure TiO_2 (P-25) was obtained from Degussa Co. Ltd. Butyltitanate, hydrofluoric acid (HF), methanol, and phenol were obtained from Shanghai Chemical Co., Ltd. RhB, methylene blue (MB), *p*-benzoquinone (BQ), isopropyl alcohol (IPA), and triethanolamine (TEOA) were all purchased from Sigma-Aldrich Inc. All chemicals were analytical grade and used without further purification.

2.2 Preparation of Square-Like TiO_2 Nanobiscuits

Typically, butyl titanate with 4.4 mL was slowly dropped into 50 mL of 5 mol/L hydrochloric acid solution, and stirred for 0.5 h. Then, 0.8 mL hydrofluoric (HF) solution (48%) was injected into the precursor solution. Next, 0.5 g of halloysite nanotubes was added to the above solution under constant stirring. Finally, the resultant solution transferred into a Teflon-lined stainless steel autoclave, followed by a solvothermal treatment at 160 °C for 12 h. After cooled to room temperature, the precipitates were washed with deionized water three times, and 0.93 g of light-yellow products were obtained after drying in a vacuum oven at 60 °C for 36 h and following calcinations at 400 °C for 5 h. For the comparison of component and morphology of products, the control experiment for the preparation of TiO_2 in the absence of halloysite nanotubes was also be carried out.

2.3 Characterization

The Brunauer–Emmet–Teller (BET) specific surface area and pore size of the samples were measured by a high speed automated area and pore size analyzer (F-Sorb3400, China). XRD patterns were analyzed with a SIEMENS Diffraktometer D5000 X-ray diffractometer using CuK_α radiation source at 35 kV, with a scan rate of 4°/s in the 2θ range of 10°–80°. The morphologies were investigated by ULTRA-55 field-emission scanning electron microscopy (FE-SEM) and JSM-2100 transmission electron microscopy (TEM) equipped with an energy dispersive X-ray spectrum (EDS, Inca Energy-200) at an accelerating voltage of 200 kV. X-ray photoelectron spectroscopy (XPS) data were obtained with an ESCALab220i-XL electron spectrometer from VG Scientific using 300 W AlK_α radiation. The base pressure was about 3×10^{-7} Pa. The binding energies were referenced to the C1s line at 284.6 eV from adventitious carbon.

2.4 Measurement of Photo-catalytic Activity

The photo-catalytic activity of TiO_2 nanobiscuits was evaluated by the photo-catalytic degradation of RhB, MB, and phenol. The photo-degradation experiments were carried out in a closed box. UV radiation source was 400 W metal halide lamp. Its wavelength range was 209–450 nm, and the peak intensity was 365 nm (model BL-GHX-V, Shanghai Bilon Instruments Co., Ltd., China). For RhB and MB, 0.005 mg of TiO_2 nanoparticles catalyst was suspended in 50 mL 10 mg/L aqueous RhB or MB solution under continuously stirring under atmosphere at room temperature. Firstly, the system was adsorbed for 0.5 h under dark condition followed by UV lamp. The sample was collected every 10 min. In the case of degradation of phenol, TiO_2 catalyst and aqueous phenol solution are 0.05 g and 50 mg/L, respectively. Every 30 min, the sample was collected and detected by gas chromatograph (model GC900A, Shanghai Tianpu Instruments Co., Ltd., China). The test method was similar to the former photo-catalytic activity tests without the change of remaining conditions.

2.5 Active Species Trapping Experiments

To detect the active species during photo-catalytic reactivity, hydroxyl radicals (·OH), superoxide radical ($O_2^{\bullet-}$), and holes (h^+) were investigated by adding 1.0 mM isopropanol (IPA) (a quencher of ·OH), BQ (a quencher of $O_2^{\bullet-}$), and TEOA (a quencher of h^+), respectively. The method was similar to the former photo-catalytic activity test.

3 Results and Discussion

Figure 1a, b presents typical FE-SEM images of as-prepared TiO_2 particles that obtained at 160 °C for 12 h. The as-synthesized TiO_2 samples are found to be regular and square-like structure with the length of side and the height around 600 and 120 nm, respectively. After calcinations treatment, the change of the samples' morphology is almost negligible, as shown in Fig. 1b. The higher magnification image shows many smaller cuboids with 50 nm in thickness that are integrally interconnected in the inner of the samples, as shown in Fig. 1c. It looks like a labyrinth that consisted of complicated series of paths or passages between the cuboids overlook at a single TiO_2 particle. By transmission electron microscopy (TEM) characterization, the roughness square-like particles with $\sim$600 nm in edge length can be observed, while the inner cores are clearly revealed by the sharp contrast between TiO_2 shells and solid interiors (Fig. 1d). The HR-TEM image of the

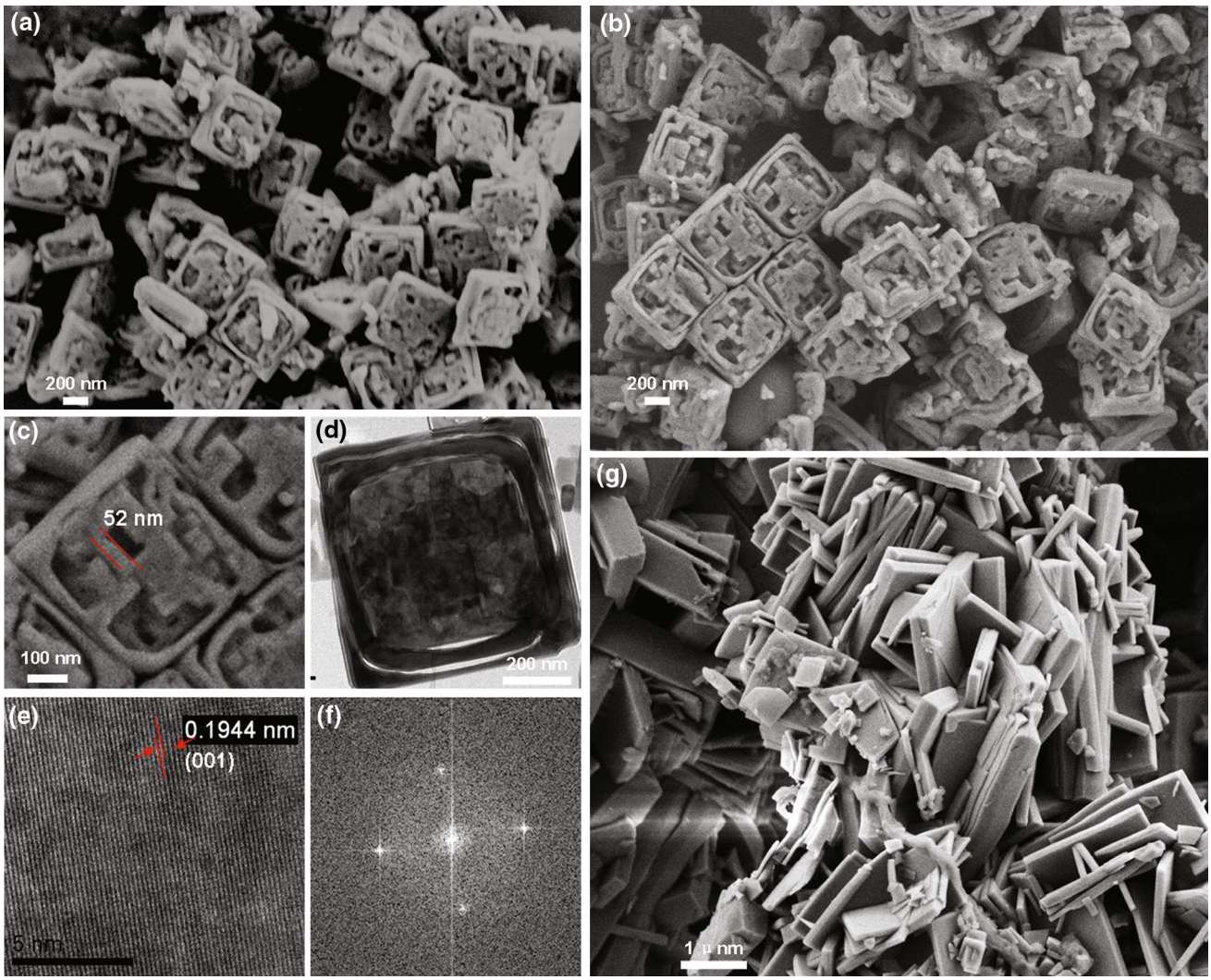

Fig. 1 SEM images of as-synthesized TiO_2 samples before **a** and after **b** calcinations treatment at lower magnification. The high magnification SEM image **c**, TEM **d**, HR-TEM images **e**, SAED pattern **f** of the samples after calcinations treatment. SEM image **g** of the products that obtained in the absence of halloysite nanotubes

samples shows a well-defined crystallinity with the lattice spacing of 0.194 nm (Fig. 1e), which is consistent with the d-spacing of the {001} plane of TiO_2 anatase phase [13]. The corresponding selected area electron diffraction (SAED) pattern reveals the single-crystalline nature of as-prepared square-like TiO_2 particles (Fig. 1f) [14, 15]. No square and biscuit-like TiO_2 particles can be found indicating the HNTs play an important role for formation of the square and biscuit-like structure (Fig. 1g). However, the exact mechanism for this is unclear.

XPS analysis can provide a valuable insight into the structure of the as-prepared products. The XPS survey spectrum of the as-prepared TiO_2 samples exhibited prominent peaks of C, O, Ti, and F, as shown in Fig. 2a. The residual carbon resulted from the organic precursors used in the sol–gel method and was not completely removed during the heat treatment. No noticeable signals assignable to Si 2p binding energy could be observed, suggesting that HNTs have been completely corroded by HF during the reaction. The concentration of F analyzed by XPS was 4.91 wt% before calcinations treatment. The peak of F 1s located at 684.7 eV was assigned to F^- ions physically absorbed on the surface of TiO_2 [16]. After the heat treatment, only the peak of F 1 s was disappeared which implied that F has been completely removed from TiO_2, as shown in Fig. 2b. The O 1s signal shows two contributions at around 529.2, 529.8, and 530.4 eV after peak modeling (Fig. 2c). The peaks at around 529.2 and 529.8 eV could be ascribed to lattice oxygen in TiO_2, while the signal at around 530.4 eV could be associated to surface hydroxyl groups. This effect confirms the progressive removal of the hydroxyl groups covering the surface of TiO_2 particles after heat treatment. The Ti 2p binding energies (Fig. 2d) of all of the samples are located at

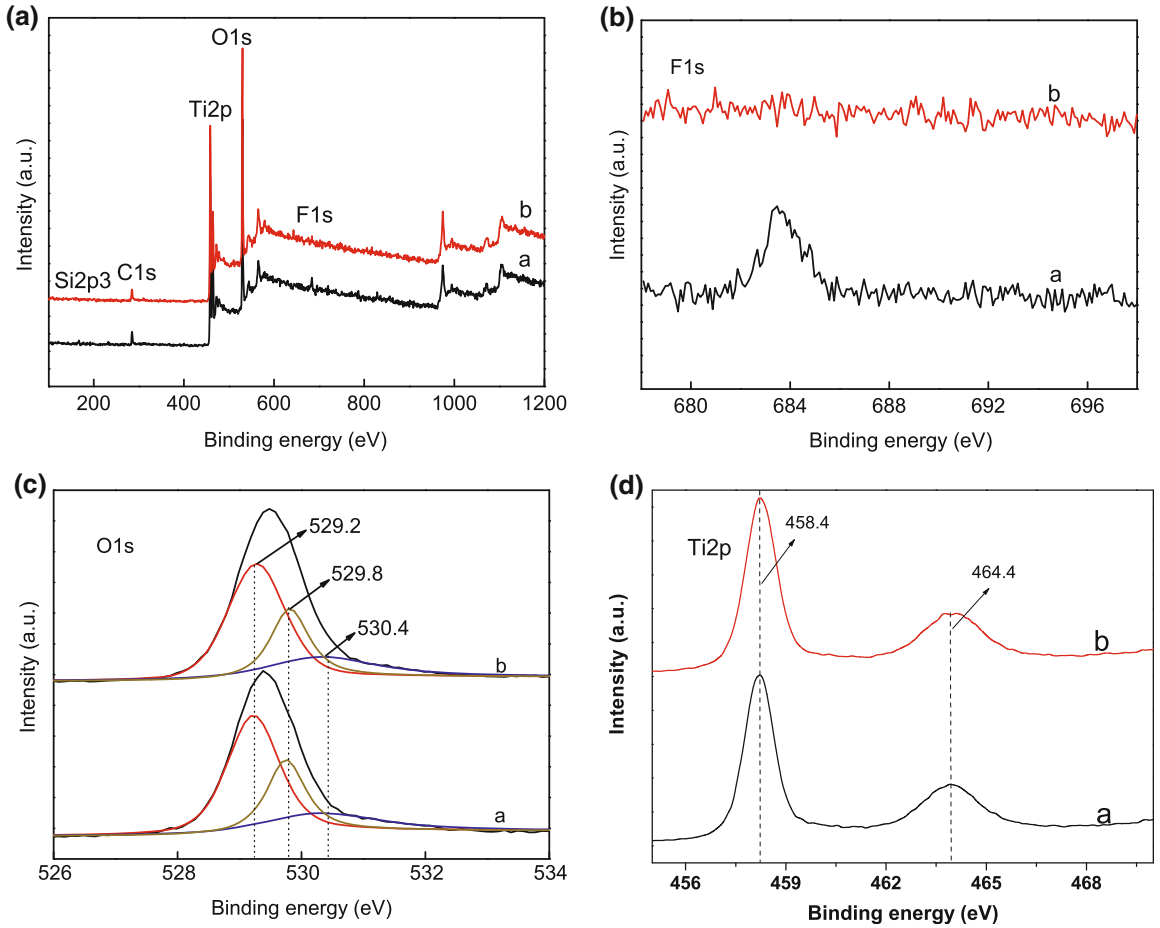

Fig. 2 XPS spectra of the as-prepared square-like TiO_2 nanobiscuits before **a** and after **b** calcinations treatment **a**, high-resolution XPS spectra of F1s **b**, O1s **c**, Ti2p **d**

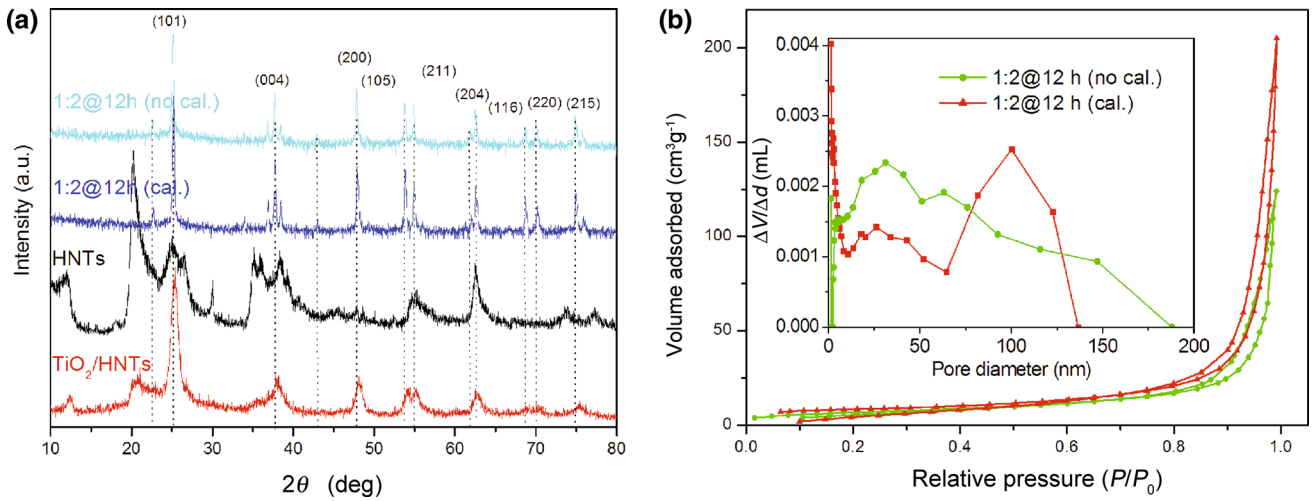

Fig. 3 XRD patterns **a**, BET specific surface area and pore size distribution curves **b** of the products

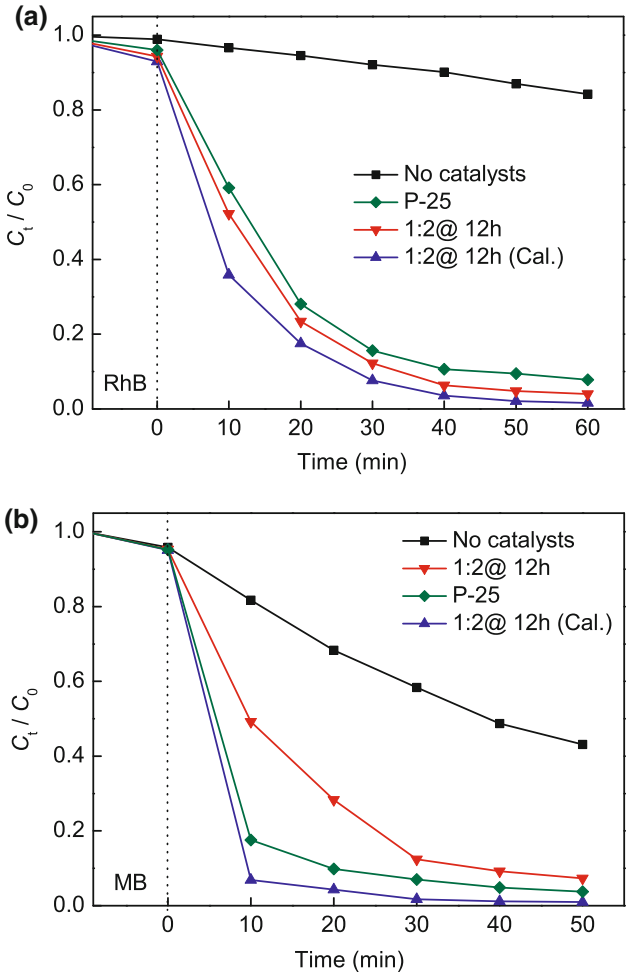

Fig. 4 The photo-catalytic degradation of RhB **a**; methylene blue (MB) **b** over square-like TiO_2 nanobiscuits under UV irradiation

around 458.4 eV (Ti 2p3/2) and 464.4 eV (Ti 2p1/2) without any shift, which are in good agreement with P-25.

For confirmation of the composition and crystallographic structure, the as-prepared TiO_2 particles are further characterized by XRD, as shown in Fig. 3a. All the diffraction peaks of as-prepared samples can be indexed to anatase phase of TiO_2 (JCPDS Card No. 21-1272) [17–19]. After the calcinations treatment, the peaks become more incisive indicating the improvement of the crystallinity of the samples. Interesting, no signals of HNTs can be found in the resultant samples which demonstrates the HNTs have been completely corroded by HF during the reaction. The as-prepared TiO_2 particles were also characterized by N_2 absorption analysis. The BET specific surface area of the calcined samples is calculated at 28.1 m^2/g which is higher than that of un-calcined samples (24.2 m^2/g) and the corresponding pore size distribution curve of the samples displays a broad pore size distribution from 1.8 to 230 nm, as shown in Fig. 3b.

To investigate the potential application of the as-prepared samples, the photo-catalytic activities of square and biscuit-like TiO_2 particles for photo-degradation of organic pollutants are investigated under UV light irradiation. As shown in Fig. 4a, for the comparison, a blank experiment is firstly carried out for indicating the self-photo-degradation of RhB ($C_0 = 10$ mg/L, $T = 300$ K). It can be found that RhB self-photo-degradation is almost negligible under light irradiation in the absence of catalyst. Compared with P-25, the decolorization rate can be accelerated in the presence of square and labyrinth-like TiO_2 particles. The photo-degradation performance of catalysts can be further improved after the calcinations treatment due to increasing crystallinity. The similar trend also can be found for photo-degradation of MB under the same conditions (Fig. 4b). However, compared with P-25, the photo-catalytic activity of as-prepared square and labyrinth-like TiO_2 is not significantly improved which may be attributed to its larger size and the resulting lower specific surface area (~ 50 m^2/g for P 25).

The photo-catalytic degradation property of colorless methanol in a liquid–solid system (5 vol%, $T = 300$ K) over the square and biscuit-like TiO_2 particles photo-catalysts is also investigated under similar conditions, as shown in Fig. 5a. The concentration change of methanol in the photo-catalytic degradation system is evaluated by the gas chromatography (GC), as shown in Fig. 5b. Before the photo-catalytic degradation, the elution time for the methanol is around 11.0 min where shows the strongest peak. With the development of photo-catalytic degradation, the intensity of peak is weakened gradually which implies the decreasing of the methanol concentration in the solution. After photo-catalytic degradation for 30 min, two new peaks with elution time at 12.7 and 8.3 min can be found. And another new peak at around 7.0 min can be observed after photo-catalytic reaction for 90 min. Only one peak with elution time at 4.9 min is present in the curve after reaction for 150 min. Based on these results, we believe that there are the various intermediates to form during the methanol decomposition because it is difficult to select just one reaction path for methanol decomposition to hydrogen, CO and CO_2. However, after reviewing several hypotheses detailed in the literature [20], there is general agreement that the dehydrogenation of methanol to CO and H_2 occurs via methoxy (CH_3O) as first intermediate, and is followed by stepwise hydrogen abstraction to CH_2O, CHO, and CO. However, the true mechanism and probability of C–O bond scission are still in some controversy.

For detecting the active species during photo-catalytic reactivity, hydroxyl radicals (·OH), superoxide radical ($O_2^{\bullet -}$), and holes (h^+) are investigated by adding 1.0 mM IPA (a quencher of ·OH), BQ (a quencher of $O_2^{\bullet -}$), and triethanolamine (TEOA, a quencher of h^+), respectively (Fig. 5c) [21]. It can be found that the photo-catalytic

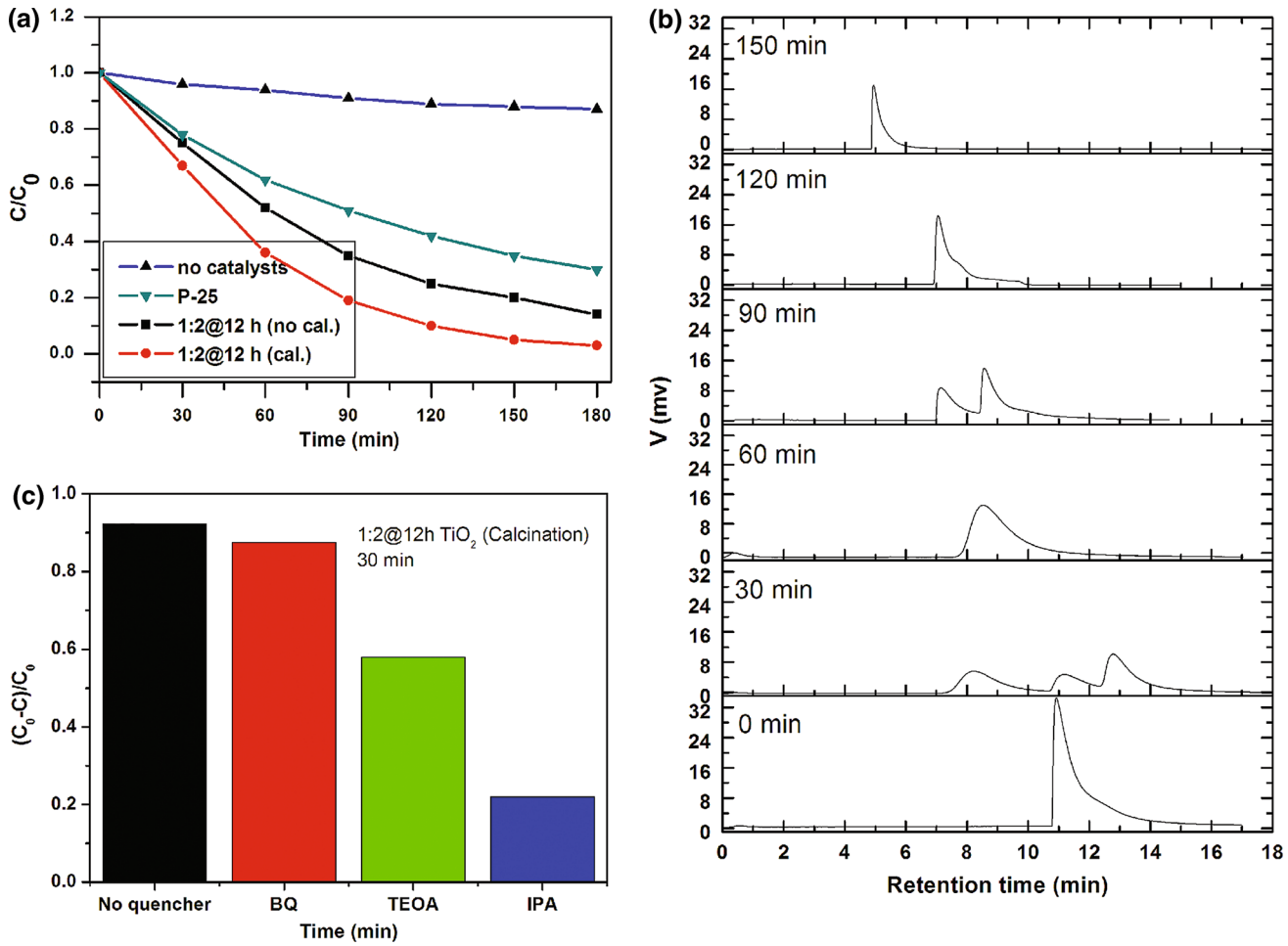

Fig. 5 The photo-catalytic degradation of methanol over square-like TiO_2 nanobiscuits under UV irradiation **a**, GC analysis **b**, a trapping experiment of active species during the photo-catalytic reaction using calcined sample as catalyst **c**

decoloration of RhB is declined slightly by the addition of 1 mM IPA. However, after addition of 1 mM BQ or 1 mM TEOA into the reaction system, the decolorization rate of RhB is decelerated significantly. The similar trend also can be found for the degradation of phenol. Therefore, it can be concluded that $O_2^{\bullet-}$ and h^+ are the main active species for degradation of organic pollutants under the UV irradiation, rather than •OH.

4 Conclusions

In summary, we have displayed a facile one-step hydrothermal method to prepare the square and biscuit-like TiO_2 particles. The as-prepared TiO_2 particles exhibit higher photo-catalytic activity than that of P-25 by evaluation the degradation of organic pollutants (RhB, MB, and phenol) under the UV light irradiation, which is resulted from the unique morphology and structure of resultant samples. These square and biscuit-like TiO_2 particles may have a bright prospect in the photo-catalytic degradation of organic contaminant.

Acknowledgments This work was financially supported by the "511 Talents Training Plan" in ZSTU, the National Natural Science Foundation of China (Nos. 51133006 and 51373155) and the Natural Science Foundation of Zhejiang Province (No. LY13B030009).

References

[1] J. Shi, J. Zheng, Y. Hu, Y. Zhao, Environ. Eng. Sci. **25**, 489 (2008)
[2] G. Jiang, R. Wang, H. Jin, Y. Wang, X. Sun, S. Wang, T. Wang, Powder Technol. **212**, 284 (2011)
[3] C.A. Castro, A. Centeno, S.A. Giraldo, S A. Mater. Chem. Phys. **129**, 1176 (2011)
[4] H.S. Kim, Y.-J. Kim, W. Lee, S.H. Kang, ACS Appl. Surf. Sci. **273**, 226 (2013)
[5] H. Zhang, G. Du, W. Lu, L. Cheng, X. Zhu, Z. Jiao, Cryst. Eng. Comm. **14**, 3793 (2012)
[6] S. Liu, J. Yu, M. Jaroniec, J. Am. Chem. Soc. **132**, 11914 (2010)
[7] J. Wang, J. Yu, X. Zhu, X. Kong, Nanoscale Res. Lett. **7**, 646 (2012)

[8] G. Jiang, X. Wang, Y. Zhou, R. Wang, R. Hu, X. Xi, W. Chen, Mater. Lett. **89**, 59 (2012)
[9] M. Zhang, K. Wada, J. Mater. Sci. Lett. **20**, 167 (2001)
[10] B. Liu, E.S. Aydil, J. Am. Chem. Soc. **131**, 3985 (2009)
[11] J.H. Park, S. Kim, A.J. Bard, Nano Lett. **6**, 24 (2006)
[12] M. Boehme, W. Ensinger, Nano-Micro Lett. **3**, 236 (2011)
[13] M. Liu, L. Piao, L. Zhao, S. Ju, Z. Yan, T. He, C. Zhou, W. Wang, Chem. Commun. **46**, 1664 (2010)
[14] X. Hu, T. Zhang, Z. Jin, S. Huang, M. Fang, Y. Wu, L. Zhang, Cryst. Growth Des. **9**, 2324 (2009)
[15] L. Shen, N. Bao, Y. Zheng, A. Gupta, T. An, K. Yanagisawa, J. Phys. Chem. C **112**, 8809 (2008)
[16] Y. Yu, H.-H. Wu, B.-L. Zhu, S.-R. Wang, W.-P. Huang, S.-H. Wu, S.-M. Zhang, Catal. Lett. **121**, 165 (2008)
[17] G. Jiang, X. Zheng, Y. Wang, T. Li, X. Sun, Powder Technol. **207**, 465 (2011)
[18] R. Wang, G. Jiang, Y. Ding, Y. Wang, X. Sun, X. Wang, W. Chen, ACS Appl. Mater. Interfaces **3**, 4154 (2011)
[19] G. Jiang, X. Wang, Z. Wei, X. Li, X. Xi, R. Hu, B. Tang, R. Wang, T. Wang, W. Chen, J. Mater. Chem. A **1**, 2406 (2013)
[20] Y. Choi, H. Stenger, Fuel Chem. Div. Prep. **47**, 723 (2002)
[21] L. Ye, J. Liu, C. Gong, L. Tian, T. Peng, L. Zan, ACS Catal. **2**, 1677 (2012)